

# **Doppler Effect Observed on the Recorded Strong Ground Motions in Iran and Turkey**

**Mehdi Zare**

Engineering Seismology Department, International Institute of Earthquake Engineering and Seismology (IIEES), Tehran, P.O.Box: 19395/3913, Iran, e-mail: mzare@dena.iiees.ac.ir

**ABSTRACT:** *The specifications of the recorded strong motions are investigated based on some selected accelerograms obtained in the Iranian and Turkish networks. The data are all recorded in the distances less than 30km to their corresponding surface fault ruptures. These records are selected based on the amplitude of the recorded acceleration, their distance to the fault and the magnitude of the earthquakes. They show, in some cases, the directivity effects based on the multiple corner frequencies observable on the Fourier spectra of the acceleration and displacement time-histories. The cases for which the records are available in the beginning and the end of the rupture, were studied to show the possible differentiation of rupture and rise times, according to the azimuthal positions of the recording stations relative to the rupture locations. The displacement pulses (width and amplitude) are different accordingly; for instance the greatest displacement pulses of Tabas record, obtained in Tabas earthquake of 16 September 1978, Mw7.4, are representative for a position in which the rupture front is approaching towards the recording site. Different studied cases in Zagros and Central Iran, as well as the records of the Turkey earthquakes (that are obtained in the nearest distances to the fault) of 17 August 1999 (Kocaeli, Mw7.4) and 12 November 1999 (Duzce, Mw7.1) indicate the rupture times differing from 2 to 10 seconds and the rise times from 0.8 to 2.85 seconds for the earthquake magnitudes of 5.9 to 7.4 and the distances to the zone of energy release varying from 5 to 30km.*

**Keywords:** Strong motions; Iran; Turkey; Acceleration; Near fault; Doppler effect; Directivity; Source time functions

## **1. Introduction**

The strong motion data in Iran and Turkey are being gathered in the national networks since 1975. The Iranian strong motion records are recorded in the national network operated by BHRC (Building and Housing Research Center) and installed in different cities and villages throughout the country. As it is outlined before [4], this network first consisted of Kinematics SMA-1 analog instruments (1975-1989), which are complemented by SSA-2 digital instruments after the Manjil earthquake of 1990. By the end of October 2001, the number of the instruments and obtained three component records were reported to be more than 1500 and 3500, respectively. The stations are mainly installed within the cities or villages for easy

operation and maintenance. A catalogue of corrected records (until 1997) for which the source parameters and the causing earthquakes are known is already published in Bard et al [4].

The first Turkish strong motion instruments were installed in 1973. Since that date, the Turkish strong motion network has grown considerably. The first instruments were of Kinematics SMA-1 type and the first recording in the epicentral region of an earthquake was obtained in Denizli from the 19 August 1976 earthquake (*mb*5.0, SW Turkey) [6]. These data are presented on the Internet since 1998 by the "General Directorate of Disaster Affairs, GDDA". These records belong to the National Strong Motion

Network that is the largest network operator in Turkey. The other available data from the Internet, are those of the Bogazici University (Kandili Observatory, Istanbul) relating to the Izmit (Kocaeli) earthquake of 17 August 1999 ( $M_w 7.4$ , CMT solution by Harvard, Seismology website, 2000m [21]). The total number of records (three component accelerograms) which were available for this study were more than 400.

Most of the available records are obtained in the hypocentral distances greater than 30km. The greater earthquakes (magnitudes greater than 6.0) and the hypo-central distances less than 30km could be the candidate for the near fault effects (the directivity effects, the presence of two corner frequencies instead of one, the existence of an important trapezoid shape on the displacement time-histories and the presence of high amplitude low frequency horizontal motions [14]). The records with mentioned conditions are very few in the strong motion databases of Iran and Turkey. The quality of the recordings imposes another limitation to select and investigate the records; the analog records contain important long period noises, due to the insufficient instability of data-logger. Investigating the directivity effects depends mostly on the existence of the records in different directions of the fault rupture, especially in the positions of the beginning and the termination of the rupture. This situation was available only in very few cases in the databases of Iran and Turkey, (mainly in the Tabas 1978 earthquake in Iran and Kocaeli and Duzce -Kaynasli- 1999 earthquakes in Turkey). The explained conditions above show different limitations existed for the present study.

In the present paper, the theory of the basic model is explained first. The criteria to select the strong motions to be studied are then discussed. The selected records are introduced further. The results are then placed in the article. The conclusions and the suggestions for the following studies come finally.

## 2. Theory of the Basic Model: the $\omega^{-\gamma}$ Model

Haskell [11] has already proposed a simple source model for the estimation of high frequency ground motions. Aki [1] and Brune [5, 6] explain the simple seismic source models. In this model, the far field displacement spectrum is characterized by a flat level  $\bar{Q}_0$  proportional to  $M_o$  at long periods, a corner frequency  $f_c$  proportional to inverse of the source dimension, and a high frequency spectral decay in the form of  $(f/f_c)^{-\gamma}$ . Taking the  $\gamma$  values as 2 or 3, we have the  $\omega$ -square or  $\omega$ -cube model, respectively

( $\omega$  is the angular frequency in radians per second, equal to  $2\pi f$ ). Hanks [13] has shown that with a  $\omega$ -square model, for which the acceleration spectra will be flat after the corner frequency, the high frequency decay may be explained by the attenuation caused by the path effects. The more complicated  $\omega$ -cube model [1], as a dynamic model, shows that the rupture nucleation generates high frequency energy, which is proportional to  $\omega^3$ . As proposed by Hanks [12], the displacement spectra may be represented by

$$\bar{Q} = \frac{\bar{Q}_0}{1 + \left(\frac{f}{f_c}\right)^\gamma}$$

Where  $\bar{Q}_0$  is the value of the flat part of the displacement spectrum, proportional to the seismic moment;  $M_o$ . For far-field S-waves, due to a double couple source embedded in an elastic, homogeneous, isotropic bounded medium, we have

$$\bar{Q}_0 = \frac{1}{4\pi R_h} \cdot \frac{M_o}{\rho} \cdot \frac{1}{\beta^3} \cdot (R'_{\theta\phi} \cdot F_s)$$

Where  $\beta$  is the shear wave velocity of the medium;  $\rho$  is the density of elastic medium; around  $(2.8 \times 10^3) \text{ kg/m}^3$ ,  $R_h$  is the hypocentral distance,  $R'_{\theta\phi}$  is the double couple radiation pattern for SH or SV waves (about 0.6 in average),  $F_s$  is the free space amplification factor (to be taken equal to 2 for the vertical incidence of the waves, and less than 2 for the local events).

The value of the flat part of the acceleration spectrum,  $A_0$ , may be related to  $\bar{Q}_0$  with  $A_0 = \bar{Q}_0 \cdot \omega_c^2$ .

Lay and Wallace [14] have shown that Doppler effects could be observed in the presence of two corner frequencies, where  $f_{c1}$  is equal to  $2/T_c$  ( $T_c$  is the rupture time or apparent rupture duration) and  $f_{c2}$  is equal to  $2/T_r$  ( $T_r$  is the rise time). Other evidence for such effects is the great displacement pulses with lowest rupture time in one end of the fault which places in front of the rupture propagation, and the lowest displacement pulse with the greatest rupture duration in the position of rupture initiation [2, 18]. Decanini et al [8] has shown that for the near-fault recorded motions for a given soil condition, the forward rupture directivity cause the arrival of the most part of the energy in a single large pulse of motion. This can result in a severe ground motion at sites towards which the fracture propagation progresses

[20, 16]. Such effects could be distinguished as well based on the existence of the long period amplification of the horizontal motions (comparing to the vertical motions; especially in the direction normal to the fault rupture). This later criteria is already observed in the Tabas earthquake where great amplifications could be observed on the horizontal motion in Tabas (placed in front of the rupture propagation) comparing to the vertical motions, especially for a site condition [22]. Decanini et al [8] indicate that the large energy demand take place in the “near-field” region (distances less than 5km to the fault). However, the condition explained by Aki and Richards [3] indicate a definition for the “near-field” conditions that could be related to a fault distance of about 30km to the fault, as well as different wave-length properties of the considered motion.

### 3. Selected Records

Ten three component records selected in this study are assigned to the major events with the magnitudes greater than  $M_w 5.7$  and in the source distances less than 30km. Decanini et al [8] represent the strong earthquakes as the events with magnitudes greater than 6.5. As it is shown in Table (1), the number of good quality records in Iran and Turkey which matches with the mentioned criteria is limited to 10 records (for the records obtained since 1975 until the end of 2000). It is notable that the signal to noise ratios are estimated for all of the studied motions as well as the  $H/V$  amplification ratio. The records with the signal to noise ratios greater than 3.0 for the frequency band of less than corner frequency ( $f_c$ ) and greater than maximum frequency ( $f_{max}$ ; that is placed at the end of the flat part of the acceleration source spectra and after which, these spectra decay) are taken to be reliable for the present study [23]. The  $H/V$  ratio is estimated to assess the fundamental frequency band for each record. When in the  $H/V$  spectral ratio, the fundamental frequency was greater than 3 for the frequency bands of greater than 15Hz, 5 to 15Hz, 2 to 5Hz, and less than 2Hz the site classes 1, 2, 3 and 4 are assigned, respectively [26].

Since the fault rupture directivity effect was aimed to be investigated, it was tried to find the records to be located at the different ends of the earthquake fault ruptures. Having these records, it was possible to observe the long period pulses on the displacement time-histories at the end of rupture and the low amplitude pulses with longer apparent duration at its beginning. This situation, however, could be found only for two records (obtained in Tabas and Deyhuk

stations) obtained in Tabas earthquake of 16 September 1978 ( $M_w 7.4$ , Figure (1)) and two other couples corresponding to the great earthquake of 1999 in Turkey (Yarima and Duzce records in Kocaeli earthquake of 17 August 1999; Figure (2),  $M_w 7.4$ ; and Duzce and Bolu records in Duzce (Kaynasli

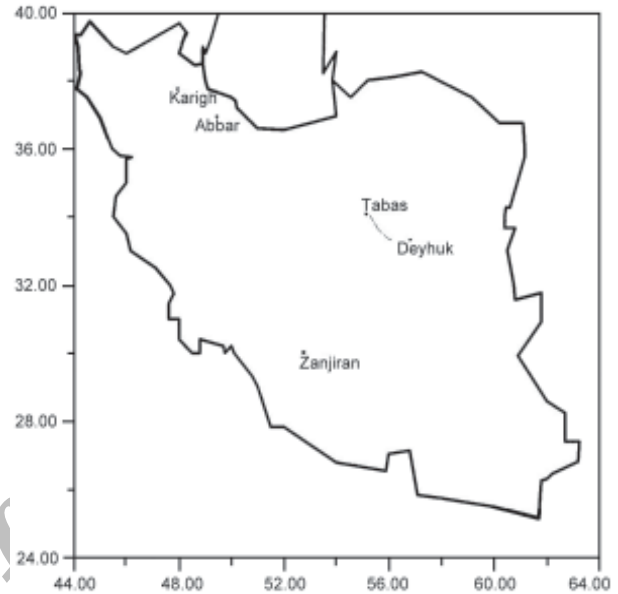


Figure 1. The location of the selected records in Iran. The location of the Tabas earthquake fault rupture is shown.

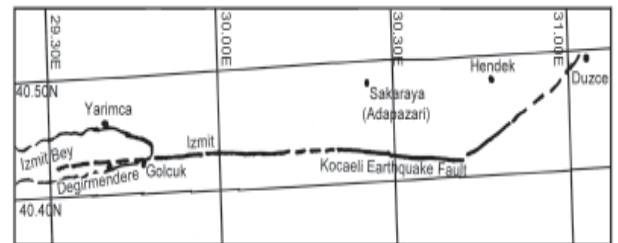


Figure 2. The fault trace of the 17 August 1999 Kocaeli earthquake, and the Yarima and Duzce stations (modified after Kandily Observatory Web Page, 2000).

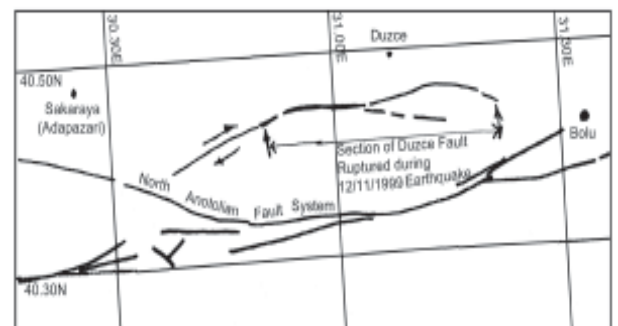


Figure 3. The fault trace of the 12 November 1999 Duzce (Kaynasli) earthquake, and the locations of Sakaraya, Duzce and Bolu stations (modified after Kandily Observatory Web Page).

**Table 1.** The specifications of the selected strong motions records for the present study and source specifications for the corresponding earthquakes. FD: Focal Depth, Dist. Epi.: Epicentral Distance, Dist. Hypo.: Hypocentral Distance, Dist. Macro. Epic.: Distance to the macroseismic epicenter (or to the surface fault rupture), focal mechanisms: RV: Reverse, SS: Strike Slip, SS/C: Strike Slip/Compressional.

No	Station	Coordinates	Code	Site	Filters (Hz) HP LP	PGA (H1) cm/sec.sec	PGA (V) cm/sec.sec	PGA (H2) cm/sec.sec	Intensity (EMS98)	Earthquake (Date)	Epicenter Coordinate	$f_{c1}$ (Hz)	$f_{c2}$ (Hz)	$F_{max}$ (Hz)	Rupture Time (sec)	Rise Time (sec)	Mw	M <sub>s</sub>	mb	M-L	FD (km)	Dist. Epi (km)	Dist. Hyp. Eptic. (km)	Dist. Macro. Epic (km)	Focal Mechanism
1	Deyhuk/ Iran	33.28N 5.7.52E	1082-1	1	0.15 25	309	176	377	VII+	16/9/1978	33.44N 56.90E	0.3	1.5	11	6.7	1.3	7.4	7.3	6.7		10	36	28	20	RV
2	Tabas/ Iran	33.67N 56.90E	1084-1	1	0.09 25	11.03	848	841	X	16/9/1978	33.44N 56.90E	0.5	1.5	6	4	1.3	7.4	7.3	6.7		10	28	27	5	RV
3	Abbar/ Iran	36.92N 48.97E	1367-1	1	0.1 25	526	548	503	VIII+	20/6/1990	36.78N 49.42E	0.4	1.9	7	5	1.05	7.3	7.7	6.8		19	43	40	8	RV/SS
4	Zanjiran/ Iran	29.10N 52.65E	1502-9	2	0.3 40	1057	993	1070	VIII	20/6/1994	29.00N 59.58E	1	2.5	22	2	0.8	5.9	5.7	5.9		9	7		7	SS
5	Karigh/ Iran	37.92N 80.05E	1833-2	3	0.08 40	578	197	572	VII+	28/2/1997	38/06N 47.11E	0.5		30	4		6.0	6.1	5.5		15	25	20		SS
6	YPT (Yarimca)/ Turkey	40.75N 29.75E	YPT22900-A- SC	1	0.15 15	218.08	235.2	309.4	VII+	17/8/1999	40.70N 29.91E	0.25	0.8	4	8	2.5	7.4	7.8	6.3	6.7	17	46	20	10	SS
7	DZC (Duzce-Met- eo)/ Turkey	40.85N 31.17E	130420A.DZC	4	0.17 17	351.6	202.6	306.9	IX+	17/8/1999	40.70N 29.91E	0.25	0.7	4	8	2.85	7.4	7.8	6.3	6.7	17	111		18	SS
8	SKR (Sakarayaa-- Bay)	40.74N 30.38E	7E0246A.SKR	3	0.25 25	193.0	153.4	333.4		11/11/1999	40.82N 30.20E	0.4	1.5	12	5	1.3	5.7	5.5	5.5	5.7	22	20	16		SS/C
9	Bol (Bolu-Bay-)/ Turkey	40.74N 31.61E	000000. BOL	4	0.2 30	729.7	193.0	795.9	VII+	12/11/1999	40.74N 31.21E	0.4	0.8	4	5	2.5	7.1	7.3	6.5	7.2	10	38	32	12	SS/C
10	DZC (Duzce Meteo)/ Turkey	40.85N 31.17E	004990A.DZC	4	0.28 20	521.3	305.9	378.1	VIII	12/11/1999	40.74N 31.21E	0.2	0.8	4	10	2.5	7.1	7.3	6.5	7.2	10	13	17	6	SS/C

earthquake of 12 November 1999; Figure (3),  $M_w$ 7.1, based on Harvard Seismology Website 2000). For other selected records, unfortunately, there was no pair to be compared in the case of one earthquake, but they are selected because they matched with above mentioned criteria. These records obtained in Abbar (20 June 1990 earthquake,  $M_w$ 7.4), Zanjiran (20 June 1994 earthquake,  $M_w$ 5.9) and Karigh (28 February 1997 earthquake,  $M_w$ 6.0) in Iran and in Sakaraya (Adapazari, 11 November 1999 earthquake,  $M_w$ 5.7) in Turkey, Figures (1) and (3) and Table (1).

### 3.1. Sources of Uncertainties

The sources of uncertainties could be the quality of recording (and/or digitization) of the accelerograms, the lack of information on the geotechnical site conditions, and the lack of the records nearby the reactivated faults. It seems that having more records with better qualities close to the capable faults, a more precise study could be performed on the observed motions in such conditions.

## 4. Results

Based on the performed processes on the selected data, the results are presented herein for each of the records and the comparisons are described in the discussions. The strong motion specifications, the site class, the applied filter, peak acceleration (after filtering) and the observed intensity are presented in Table (1). The

earthquake source specifications (epicenter location, Magnitude scales, and the values for different distance definitions, focal depth and mechanisms) as well as the corner and maximum frequencies and the values of rise and rupture times are given in Table (1) for the mentioned 10 selected records.

### 4.1. Fast Fourier Transformation of Acceleration and Displacement for Filtered Records

The FFT's of the accelerations and displacements are plotted for the selected records of Deyhuk; Figure (4), Tabas; Figure (5), Abbar; Figure (6), Zanjiran; Figure (7), Karigh; Figure (8), Yarimca; Figure (9), Duzce (17 August 1999 record; Figure (10)), Sakaraya; Figure (11), Duzce (12 November 1999 record, Figure (12), and Bolu, Figure (13)). The different corner frequencies ( $f_{c1}$  and  $f_{c2}$ ) and  $f_{max}$  are shown in the mentioned figures. The first corner frequency ( $f_{c1}$ ) for Tabas is higher than Deyhuk and correspondingly rupture time in Tabas is lower, Figures (4) and (5), Table (1). The rupture time of 1sec for Zanjiran record, Figures (7b) and (7d), Table (1), obtained in Zagros belt) is lower than the values obtained in Alborz and Central Iran (Abbar, Tabas, Deyhuk, Karigh, Table (1). The corner frequencies and the rupture times are observed to be the same for two recorded motions of Yarimca and Duzce during the 17 August 1999 earthquake, which were placed in two different sides of the fault rupture, see Figure (2). Zare [24] has discussed the

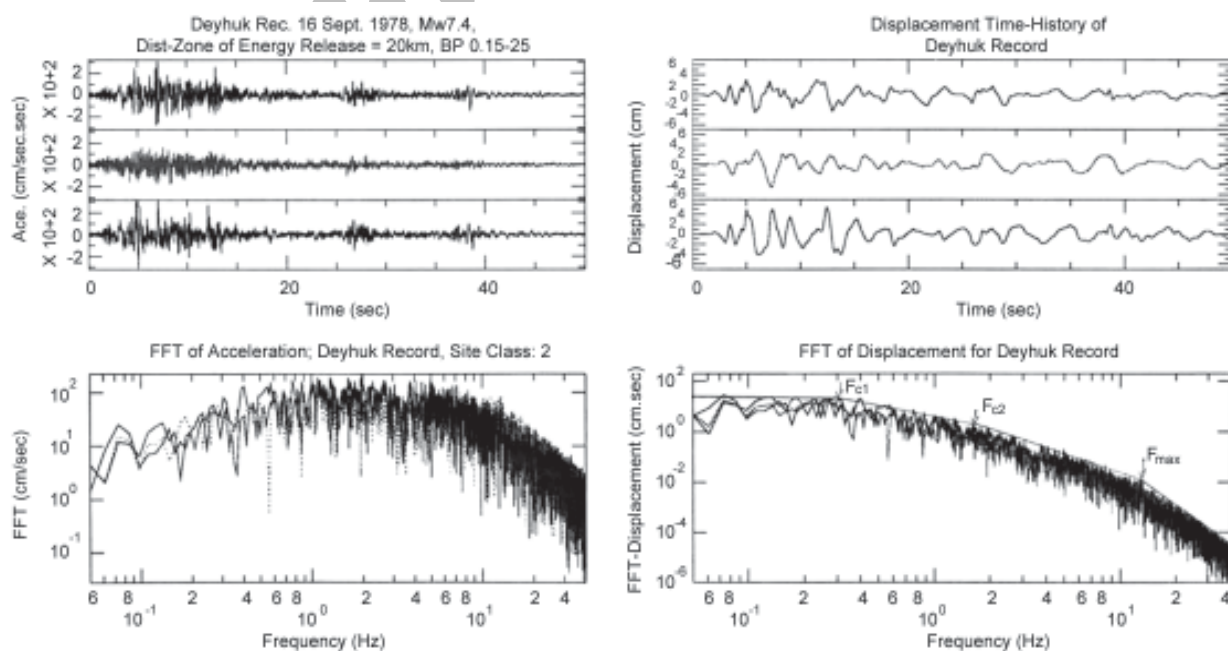


**Figure 4.** The Deyhuk record; (a) The filtered accelerogram, (b) The FFT of accelerations, (c) The displacement time-history and (d) The FFT of displacement, where the  $f_{c1}$ ,  $f_{c2}$  and  $f_{max}$  are shown in the figure. The upper and lower figures are the horizontal components and the middle one corresponds to the vertical component.

possibility of bilateral directivity effects in the Kocaeli earthquake of 17 August 1999. Such effect could be considered with the equal pulse shapes, frequency contents and corner frequencies (and therefore rupture times) in these two records in opposite ends of the Kocaeli fault rupture. These are the effects of the extended finite sources in the

mentioned events.

The double corner frequencies are observable for the case of Abbar strong motions (Manjil earthquake) as well Figures (6b) and (6d). This record could not be compared with another strong motion to be obtained in another end of the fault rupture (Abbar station was located in one end of the Manjil earthquake fault

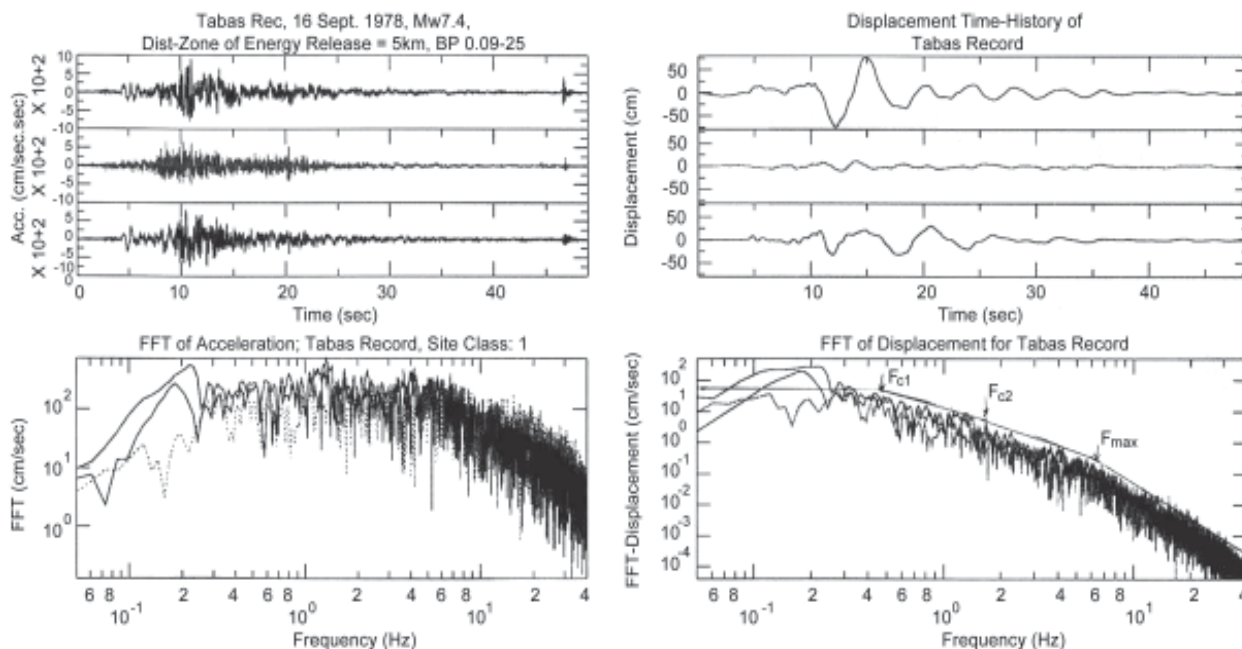


**Figure 5.** The Tabas record; (a) the filtered accelerogram, (b) the FFT of accelerations, (c) the displacement time-history and (d) the FFT of displacement, where the  $f_{c1}$ ,  $f_{c2}$  and  $f_{max}$  are shown in the figure. The upper and lower figures are the horizontal components and the middle one corresponds to the vertical component.

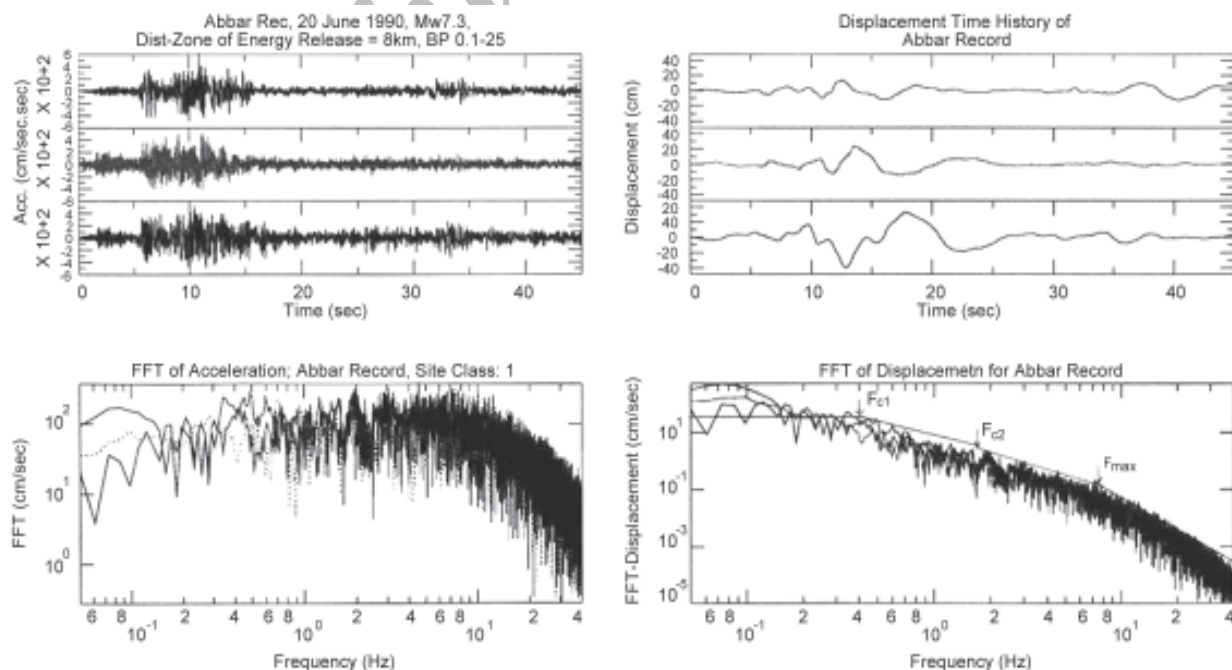


**Figure 6.** The Abbar record; (a) the filtered accelerogram, (b) the FFT of accelerations, (c) the displacement time-history and (d) the FFT of displacement, where the  $f_{c1}$ ,  $f_{c2}$  and  $f_{max}$  are shown in the figure. The upper and lower figures are the horizontal components and the middle one corresponds to the vertical component.

rupture, see Figure (1). The Karigh accelerogram that is recorded in 28 February 1997 earthquake in NW Iran [25] was investigated as well but only one corner frequency could be observed.

The values of  $f_{max}$  do not show any systematic change in the available studied records. The only great change of  $f_{max}$  values in different ends of the fault

rupture could be assigned to the case of Tabas and Deyhuk, where the value of  $f_{max}$  in Tabas has moved more or less towards the lower frequencies (6Hz, comparing to the  $f_{max}$  observed for Deyhuk records; 11Hz). In the other case of a pair of records Duzce (Kaynashli) earthquake of 12 November 1999; Duzce and Bolu record), the same values of  $f_{max}$  are more or

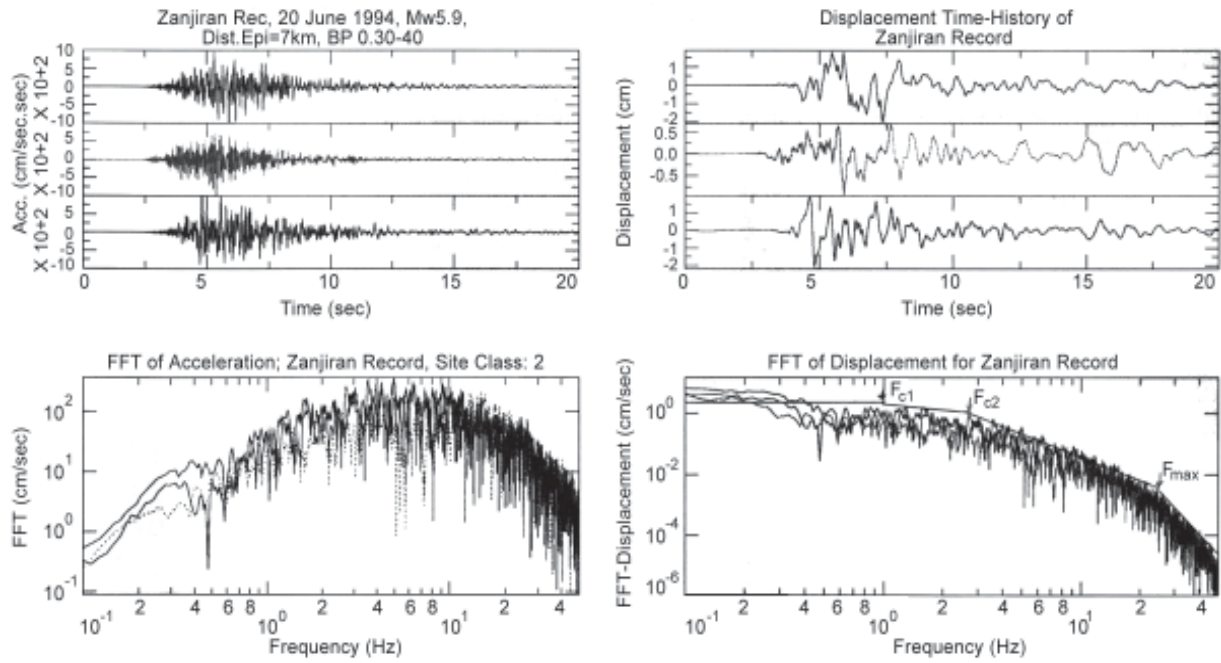


Figure 7. The Zanjiran Record; (a) the filtered accelerogram, (b) the FFT of accelerations, (c) the displacement time-history and (d) the FFT of displacement, where the  $f_{c1}$ ,  $f_{c2}$  and  $f_{max}$  are shown in the figure. The upper and lower figures are the horizontal components and the middle one corresponds to the vertical component.

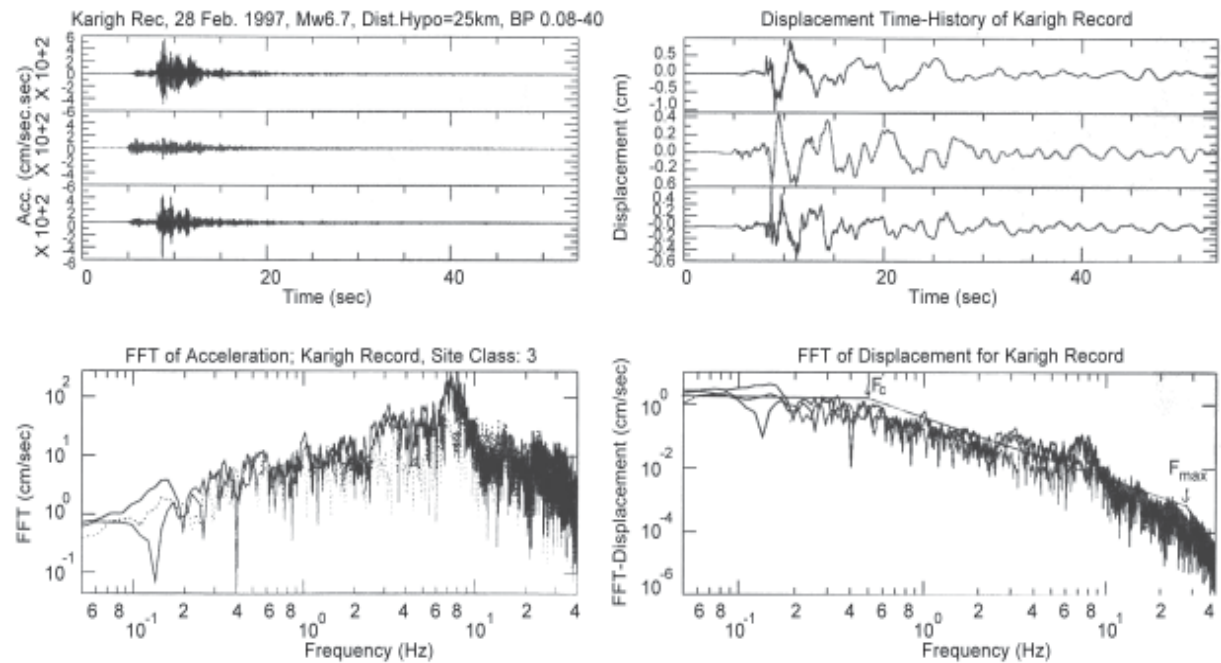


Figure 8. The Karigh Record; (a) the filtered accelerogram, (b) the FFT of accelerations, (c) the displacement time-history and (d) the FFT of displacement, where the  $f_{c1}$ ,  $f_{c2}$  and  $f_{max}$  are shown in the figure. The upper and lower figures are the horizontal components and the middle one corresponds to the vertical component.

less evident. The variations of  $f_{max}$  could be studied having more data, due to the high frequency attenuation of strong motions.

#### 4.2. Waveform of the Displacement Time-Histories

The displacement time-histories (DTH) are obtained

based on the double integration of the acceleration records. The greater pulses on Tabas DTH comparing to that of Deyhuk could be taken as a pulse induced by directivity effects, Figures (4) and (5). The Abbar DTH (Figure (6)) had no pair to be compared, because no record obtained in the middle parts (Manjil; the

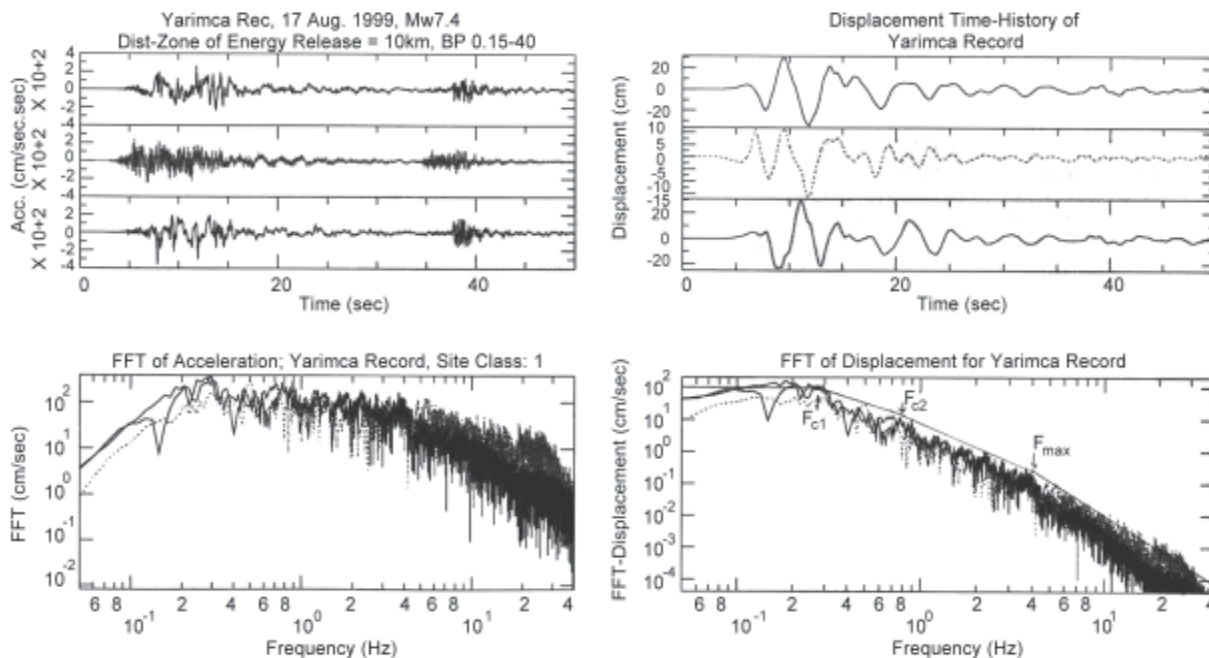


**Figure 9.** The Yarimca record; (a) the filtered accelerogram, (b) the FFT of accelerations, (c) the displacement time-history and (d) the FFT of displacement, where the  $f_{c1}$ ,  $f_{c2}$  and  $f_{max}$  are shown in the figure. The upper and lower figures are the horizontal components and the middle one corresponds to the vertical component.

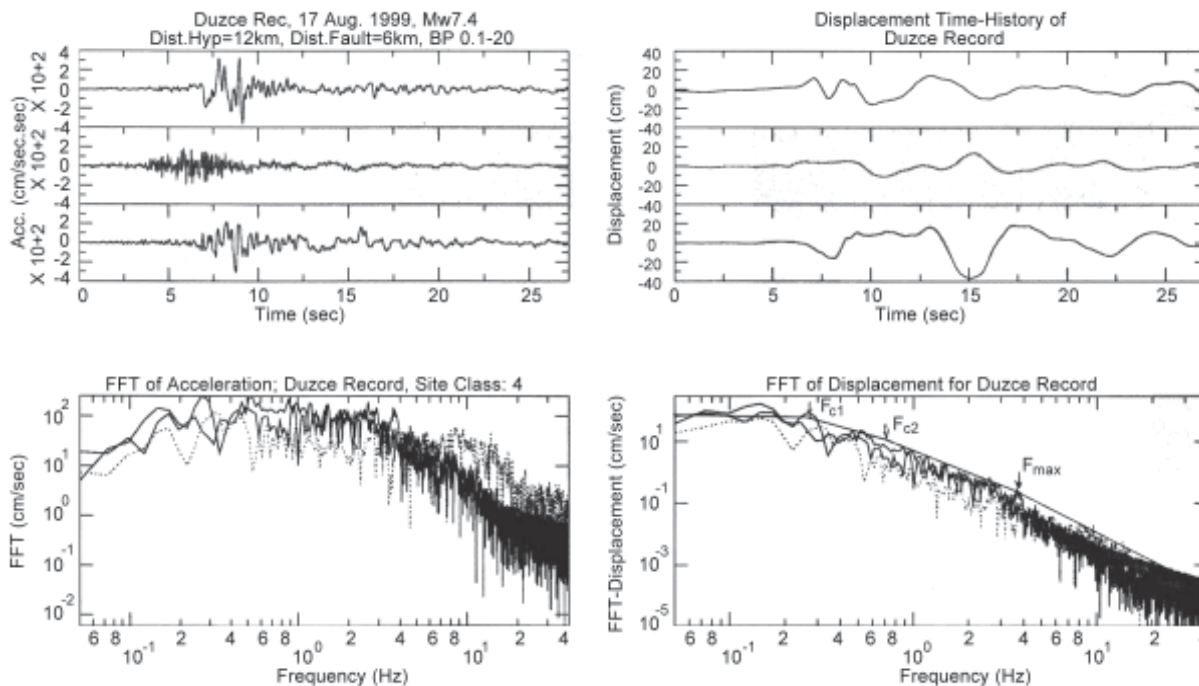


**Figure 10.** The Duzce record (of 17/08/1999 earthquake); (a) the filtered accelerogram, (b) the FFT of accelerations, (c) the displacement time-history and (d) the FFT of displacement, where the  $f_{c1}$ ,  $f_{c2}$  and  $f_{max}$  are shown in the figure. The upper and lower figures are the horizontal components and the middle one corresponds to the vertical component.



instrument in Sefid-Rud dam was off at the time of the Manjil earthquake, because of the lack of battery) or in the other end of the Manjil earthquake fault. The lack of information was similar for Zanjiran, Figure (7) and Ardebil, Figure (8) earthquake records.

The great pulses in Yarimca and Duzce *DTH*'s-

Figures (9) and (10) - are similar (Kocaeli earthquake of 17 August 1999). The Sakaraya (Adapazari) *DTH*'s (Figure (11) of 11 November 1999 earthquake had no pair nearby the fault, to be compared. For this case, it was interesting to observe greater amplitude of displacements on the first horizontal (north-south

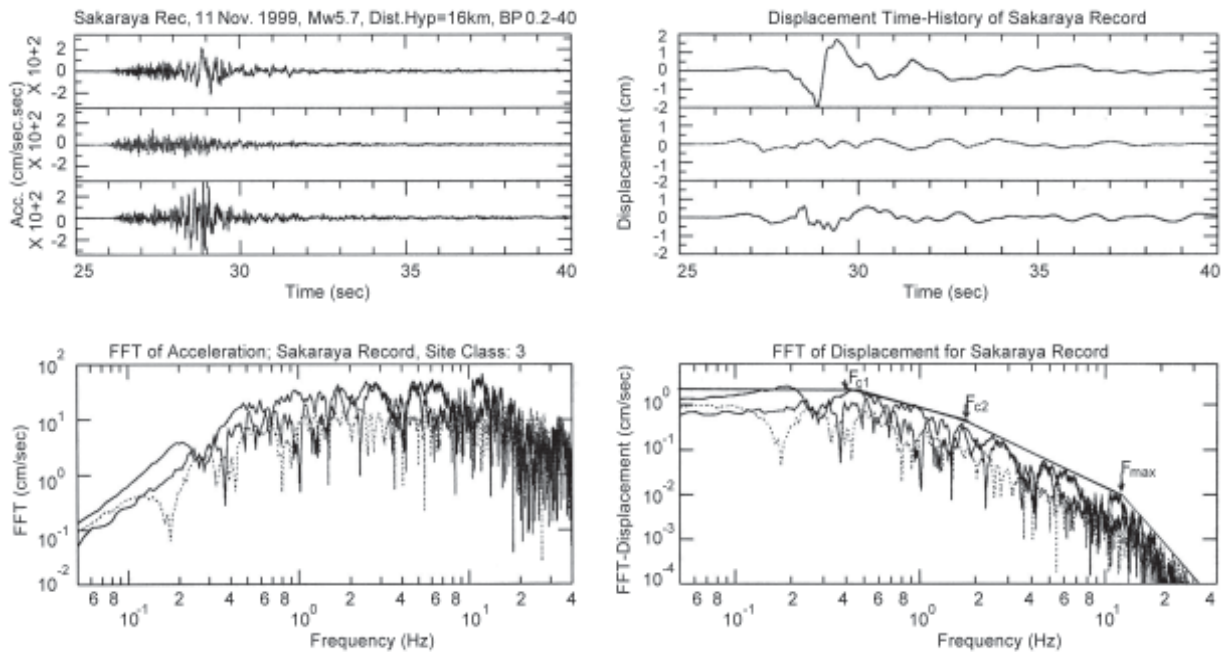


**Figure 11.** The Sakaraya (Adapazari) record; (a) The filtered accelerogram, (b) the FFT of accelerations, (c) the displacement time-history and (d) the FFT of displacement, where the  $f_{c1}$ ,  $f_{c2}$  and  $f_{max}$  are shown in the figure. The upper and lower figures are the horizontal components and the middle one corresponds to the vertical component.

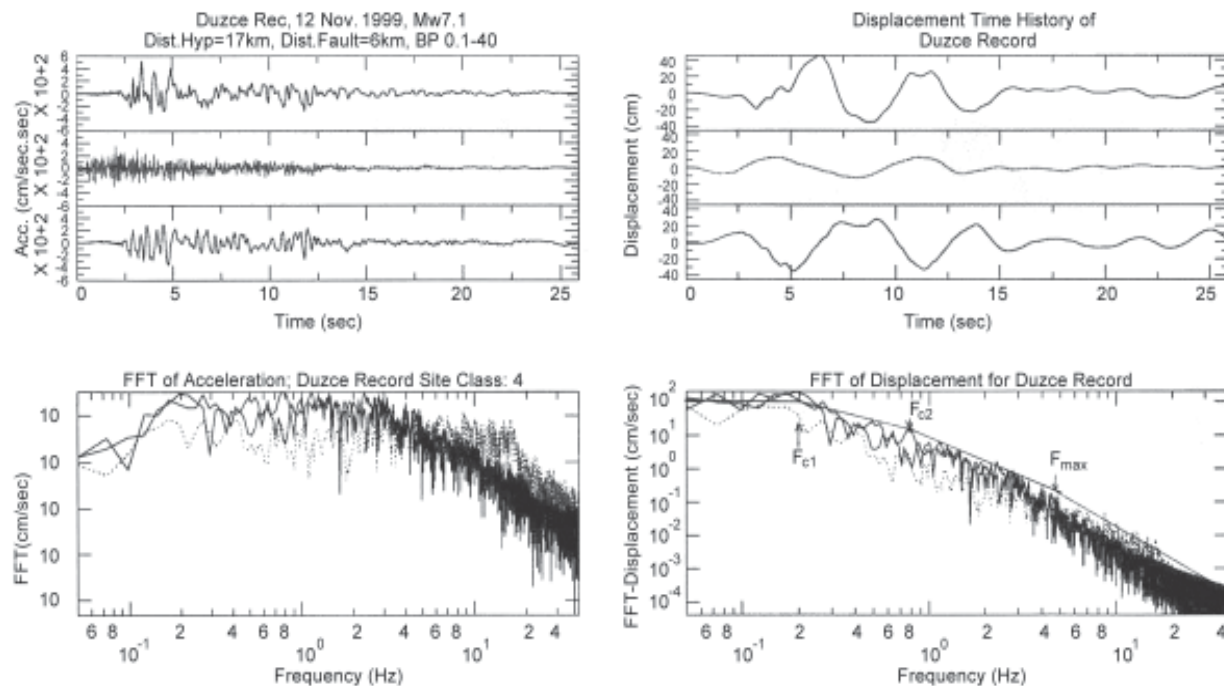


**Figure 12.** The Duzce record (of 12/11/1999 earthquake); (a) the filtered accelerogram, (b) the FFT of accelerations, (c) the displacement time-history and (d) the FFT of displacement, where the  $f_{c1}$ ,  $f_{c2}$  and  $f_{max}$  are shown in the figure. The upper and lower figures are the horizontal components and the middle one corresponds to the vertical component.

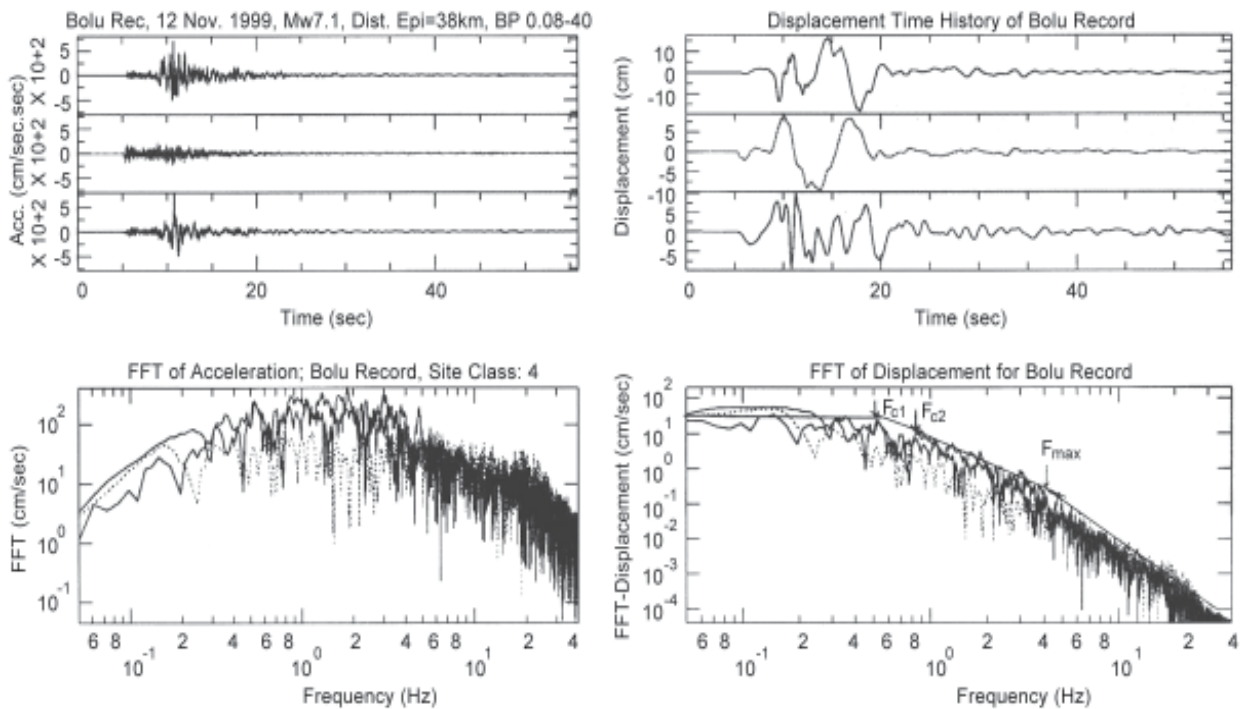


**Figure 13.** The Bolu record; (a) The filtered accelerogram, (b) the FFT of accelerations, (c) the displacement time-history and (d) the FFT of displacement, where the  $f_{c1}$ ,  $f_{c2}$  and  $f_{max}$  are shown in the figure. The upper and lower figures are the horizontal components and the middle one corresponds to the vertical component.

direction) relative to the second horizontal component (on east-west direction). The *DTH*'s of Duzce and Bolu (12 November 1999 earthquake, see Figures (12) and (13)), indicate the greater displacements in Duzce. This problem is discussed further in this article.

## 5. Discussion

The earthquake of Tabas (16/06/1978, central Iran), Kocaeli (17/08/1999,  $M_w$ 7.4 Marmara Sea region, NW Turkey) and Kaynasli (12/11/1999,  $M_w$ 7.1, Bolu area, NW Turkey) are selected to be discussed. This selection was based on the availability of a pair of records obtained in opposite ends of the earthquake fault rupture.

❖ The *FFT* of the amplitudes displacements are compared for different components of Tabas and Deyhuk records in Figure (14). The greater amplitudes for Tabas record is evident, while the  $f_{c1}$  and  $f_{c2}$  are placed in different frequencies (this figure should be compared with Figures (4) and (5)). Tabas was much closer to the active part of the rupture than Deyhuk, and the rupture propagation towards Tabas is supported by the observed much higher  $f_{c1}$  in this station. The displacements for the first 20 seconds of the *DTH*'s in Tabas and Deyhuk are compared however in Figure (15). A great

difference is observable between these two records; the evident greater amplitudes and even the trapezoid type pulses in about 16 to 18 seconds correspond to Tabas *DTH*. This could be interpreted to the rupture directivity towards the Tabas, during the Tabas earthquake.

❖ The *FFT* of the amplitude of displacements for different components of Yarimca and Duzce records are compared in Figure (16). The shapes of these spectra are more or less similar in different frequencies. This similarity could be followed in the waveform of the *DTH*'s of these two records, see Figure (17). This is suggested to be related to the bilateral directivity in the Kocaeli earthquake. According to Tibi et al [21], the rupture velocity is taken to be  $4.5\text{km/sec}$  in the Kocaeli earthquake. Based on the estimated rupture times for the Kocaeli earthquake in this paper, this would result to the rupture lengths of about  $36\text{km}$  for Kocaeli earthquake. It can not be related to the  $125\text{km}$  observed total ruptures length during the mentioned earthquake, but it may correspond to the rupture length of one part of the total fault segments. This could be justified in Figure (10), in which the displacement record of the Kocaeli earthquake recorded in Duzce station is shown. The trapezoid shapes are evident both for *P* and *S* waves, which

means that this station could record only part of the total rupture (maybe the eastern most part only). The corner frequency  $f_{c1}$  of 0.25Hz indicates that the *S* wave dominates in the spectrum. However the displacement estimated in Yarimca (Figure (9)) is more complicated, which is probably to be dominated by the *S* wave as well.

- ❖ The *FFT* of the amplitudes of displacements in Duzce and Bolu records are compared for different components in Figure (18). The level of the Fourier amplitude of displacements in Duzce shows greater values than that of Bolu (it should be compared with Figures (12) and (13)). The wave forms of *DTH*'s for these two locations are compared in Figure (19), where the difference is evident especially for the horizontal components; the displacements were greater in Duzce, but the rupture time was found to be shorter in Bolu. Based on a rupture velocity of 2km/sec for Duzce earthquake [21] the rupture lengths of 48km and 24km for the rupture time estimations in Bolu and Duzce, could be found, respectively, which seems however to be reasonable according to the observed fault segment. Tibi et al [21] believe on a bilateral directivity for the Duzce earthquake as well. Referring to the Duzce (Kaynaşli) fault rupture location Figure (3), it seems that Duzce was not in a location to be in front of the rupture propagation. It is probable that Duzce was located outside of the development of rupture front, but the long period pulses are indicative for a directivity effect, probably in the middle parts of the fault. However, Milkereit et al [19] represent an epicenter location much closer to the Duzce station, and according to their estimation, the rupture is started at a depth of about 12.5km and propagated bilaterally both towards the east and west and from greater to shallower depths. Therefore the directivity effects should be observed at Duzce station, as well. This problem can be investigated in the future.

## 6. Conclusions

The present study has shown the importance of the Doppler effects in the earthquakes occurred in the last 25 years in Iran and Turkey. The location of the cities and the industrial localities nearby the border of the mountains and plains (where there are the capable

places for quaternary and active faults) in these countries impose an additional attention to be paid to the source directivity problems in the seismic resistant designs. The conclusions could be summarized as follows:

- ❖ This study showed the impression of the rupture directivities on the corner frequencies and the displacement pulse shapes for the motions recorded in different directions due to the fault rupture. The records obtained in front of the rupture developments showed shorter apparent rupture duration (rupture time) with greater pulses, than those located in the opposite side.
- ❖ The values of two corner frequencies for most of the studied records indicate the variations of rise time and rupture time for the studied records. The second corner frequencies (and correspondingly; the rise times) seems to be less stable for a pair of motions obtained in the opposite sides of a fault, but the first corner frequency (and correspondingly; the rupture times) show important differences.
- ❖ The displacement pulses are different according to the locality of the obtained motion; the motions recorded in front of the rupture propagation indicate greater pulses (sometimes the trapezoids) comparing to the opposite side motions.
- ❖ For the motions recorded in Turkey, the comparison of north-south and east-west horizontal components of the records was possible. Among the studied records, the most important difference was observable in the case of Sakaraya (Adapazari) records in 11 November 1999 earthquake (with greater pulses on the north-south direction). Other records do not represent any important difference between these two directions.

Based on the preformed study, the suggestions for the continuation of researches on the near field strong motions could be listed as follows:

- ❖ More dense arrays should be installed around the major active faults of the region. This can provide more comprehensive data set to be studied in the case of a great earthquake.
- ❖ The sensors of the horizontal two components of the installing instruments should be directed either towards the north and the east (or one component parallel to and another one normal to the fault direction).

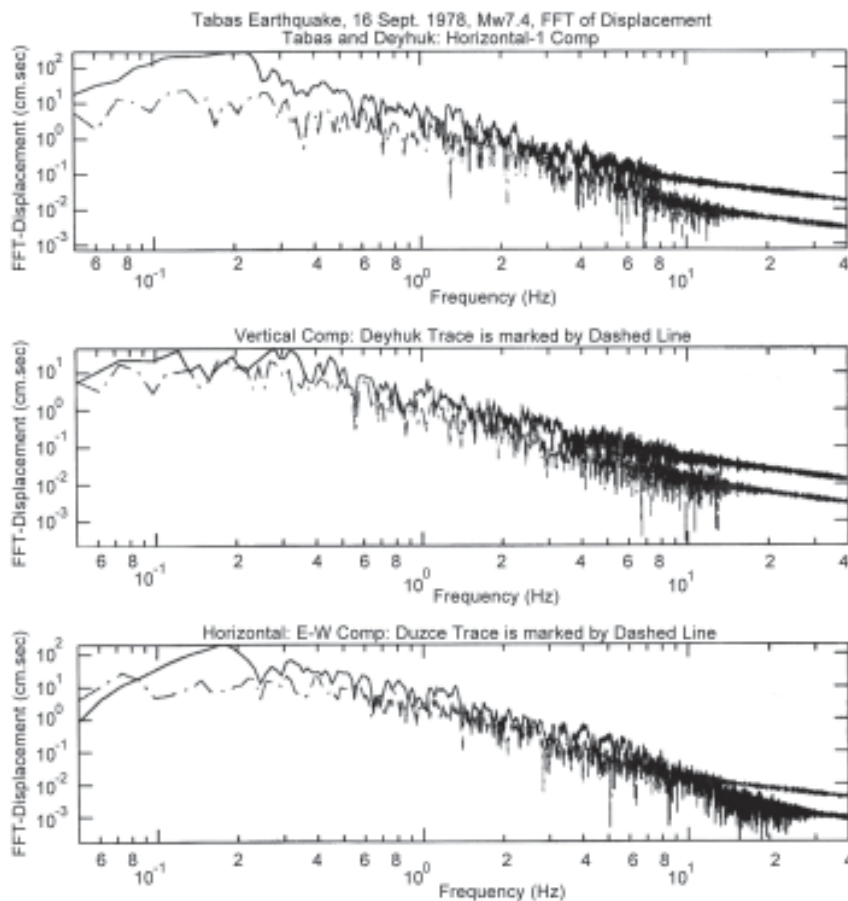


**Figure 14.** The FFT of displacements are compared for Tabas and Deyhuk records for different components: the upper and lower are the horizontal components and the middle one is the vertical component (the Deyhuk traces are shown with dashed lines).

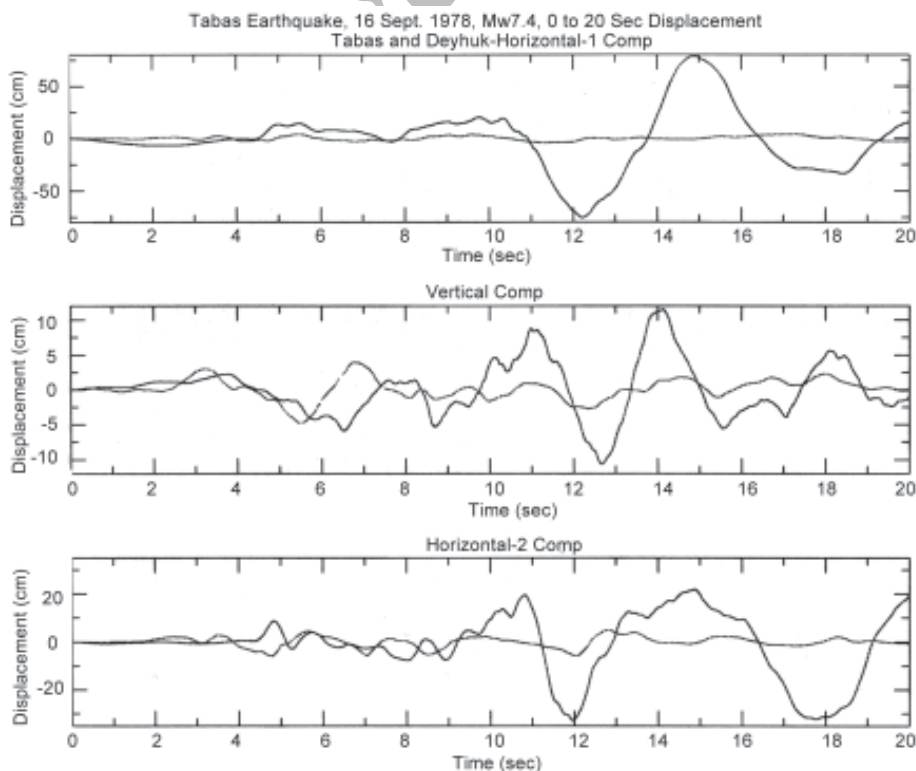


**Figure 15.** The displacement time-histories are compared for Tabas and Deyhuk records for different components: the upper and lower are the horizontal components and the middle one is the vertical component (the Deyhuk traces are shown with dashed lines).

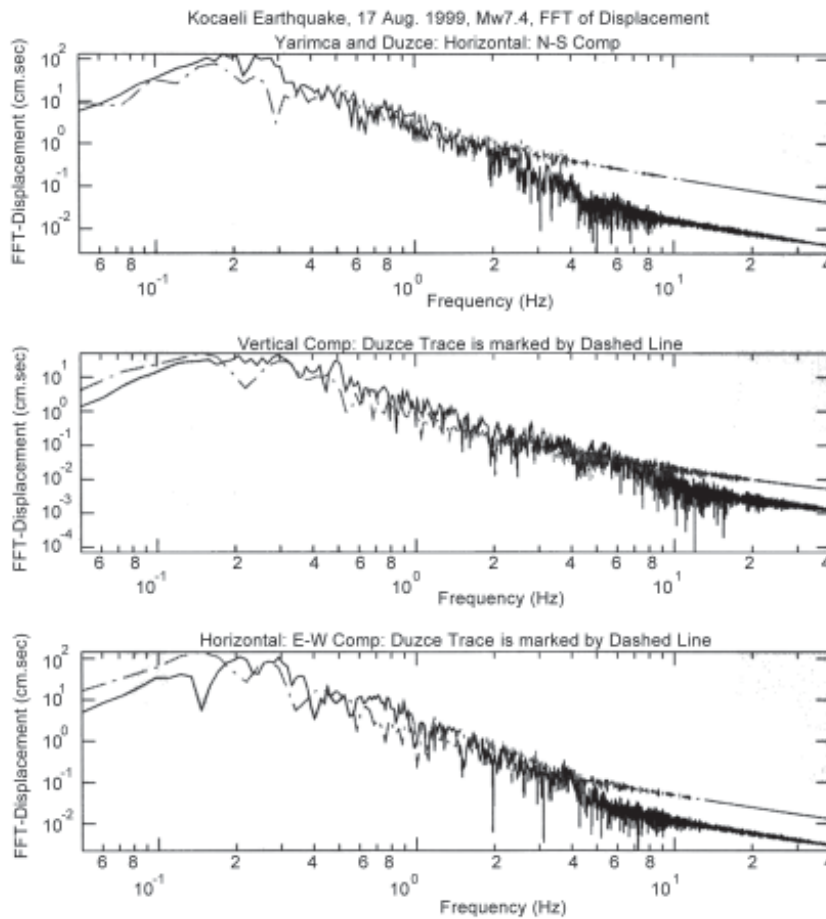


Figure 16. The FFT of displacements are compared for Yarimca and Duzce records for different components: the upper and lower are the horizontal components and the middle one is the vertical component (the Duzce traces are shown with dashed lines).

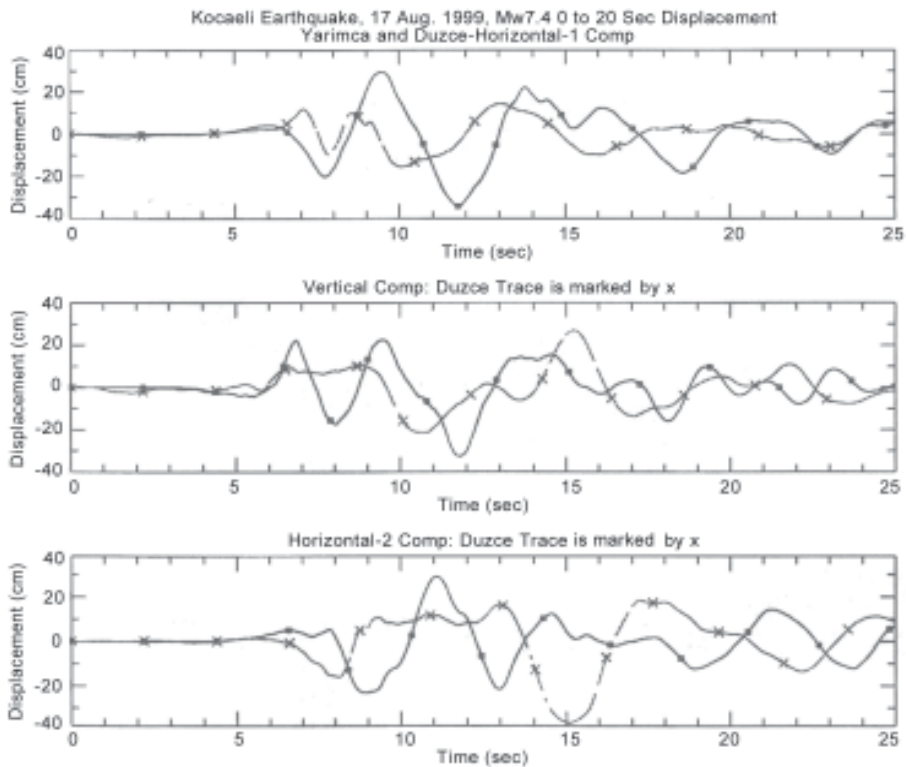


Figure 17. The displacement time-histories are compared for Yarimca and Duzce records for different components: the upper and lower are the horizontal components and the middle one is the vertical component (the Duzce traces are shown in dashed lines).

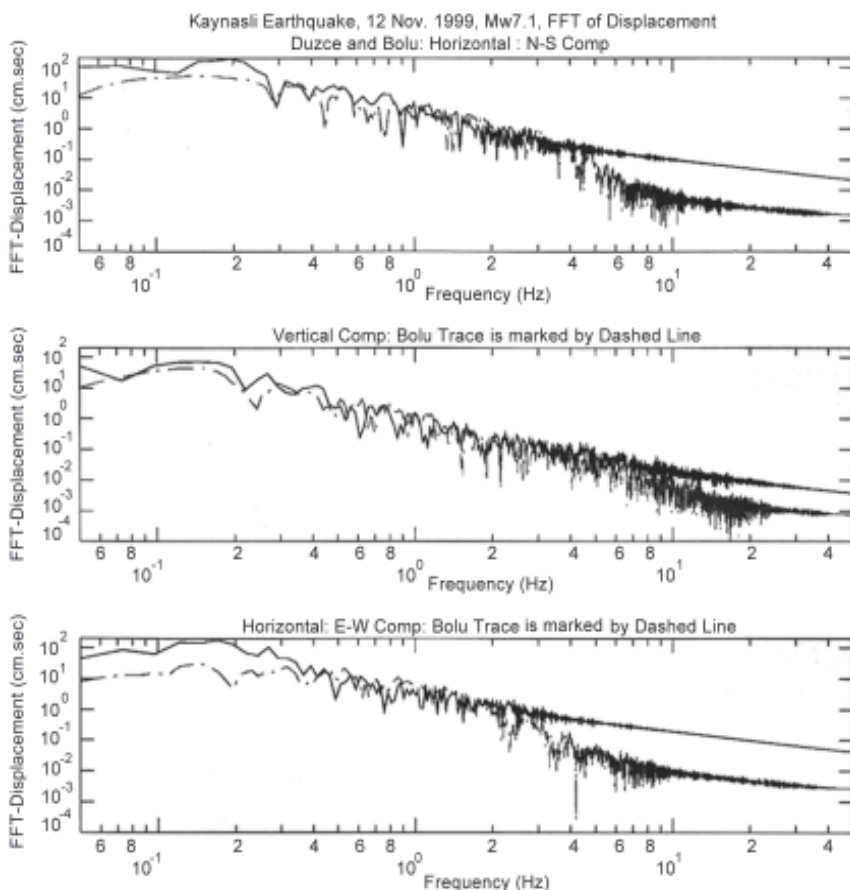


Figure 18. The FFT of displacements are compared for Duzce and Bolu records for different components: the upper and lower are the horizontal components and the middle one is the vertical component (the Bolu traces are shown with dashed lines).

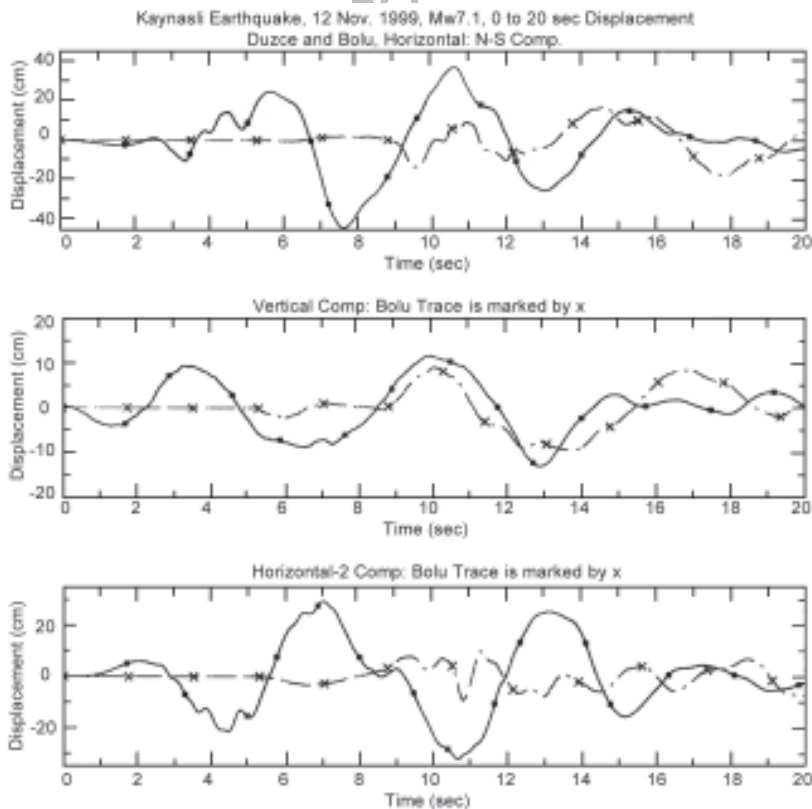


Figure 19. The displacement time-histories are compared for Duzce and Bolu records for different components: the upper and lower are the horizontal components and the middle one is the vertical component (the Bolu traces are shown with dashed lines).

- ❖ In the future earthquake resistant designs for the engineering purposes, where the site is located nearby a fault, it is suggested to pay attention to the near fault recorded motions.

### Acknowledgments

The records of the Iranian earthquakes used in this study was provided by the Building and Housing Research Center (BHRC), the organization who maintain and provide such information in Iran, which is dully acknowledged. The General Directorate of Disaster Affairs of Turkey, as well as the Kandily Observatory of the Bogazici University in Istanbul, have released the strong motion information of Turkey on the internet, that is appreciated as well. The author is grateful to Dr. Hossein Hamzehloo of IIEES for the useful discussions and suggestions. The author appreciates the comments and corrections proposed by Dr. M. Mokhtari of IIEES and three anonymous external referees, which helped in improving the quality of the paper.

### References

1. Aki, K. (1967). "Scaling Law of Seismic Spectrum", *J. Geoph. Res.*, **72**, 1217-1231.
2. Aki, K. (1968). "Seismic Displacements Near a Fault", *J. Geoph. Res.*, **73**, 5359-5375.
3. Aki, K. and Richards, P.G. (1980). "Quantitative Seismology, Theory and Methods", **1**, W.H. Freeman and Co. San Francisco.
4. Bard, P.-Y, Zare, M., and Ghafory-Ashtiany, M. (1998). "The Iranian Accelerometric Data Bank, A Revision and Data Correction", *Journal of Seismology and Earthquake Engineering*, **1**(1), 1-22.
5. Brune, J.N. (1970). "Tectonic Stresses and the Spectra of Seismic Shear Waves", *J. Geoph. Res.*, **75**, 4997-5009.
6. Brune, J.N. (1971). "Corrections", *J. Geoph. Res.*, **76**, 5002pp.
7. Can Ates, R.N. and Bayulke, N. (1982). "The 19 August 1976 Denizli, Turkey, Earthquake: Evaluation of the Strong Motion Accelerograph Record", *Bull. of the Seismological Soc. of America*, **72**(5), 1635-1649.
8. Decanini L., Mollaioli, L., Panza, F.F., Romanelli, F., and Vaccari, F. (2001). "Probabilistic VS Deterministic Evaluation of Seismic Hazard and Damage Earthquake Scenarios: A General Problem, Particularly Relevant for Seismic Isolation", *Proc. 7<sup>th</sup> Int. Seminar on Seismic Isolation, Passive Energy Dissipation and Active Control of Vibrations of Structures*, Assisi, Italy, (under publication).
9. Frankel, A. (1991). "High-Frequency Spectral Falloff of Earthquakes, Fractal Dimension of Complex Rupture, b Values, and the Scaling of Strength on Faults", *J. Geoph. Res.*, **96**(B4), 6291-6302.
10. General Directorate of Disaster Affaires, Web-Site, 2000, <http://angora.deprem.gov.tr/>.
11. Haskell, N.A. (1964). "Total Energy and Energy Spectral Density of Elastic Wave Radiation from Propagating Faults", *Bull. Seismol Soc. of America*, **54**, 1811-1841.
12. Hanks, T.C. (1979). "b Value and  $\omega^{-\gamma}$  Seismic Source Models: Implications for Tectonic Stress Variations Along Active Crustal Fault Zones", *J. Geoph. Res.*, **84**, 2235-2242.
13. Hanks, T.C. (1982). " $f_{max}$ ", *Bull. Seismol Soc. of America*, **72**, pp1867-1880.
14. Lay, T. and Wallace, T.C. (1995). "Modern Global Seismology", Academic Press Inc.
15. Harvard University, Seismology Dept. Web site, 2000, <http://www.seismology-harvard.edu/>.
16. Heaton, T.H., Hall, J.F., Wald, D.J., and Halling, M.W. (1995). "Response of High Rise and Base Isolated Buildings to Hypothetical  $M_w$  7.0 Blinde Thrust Earthquake", *Science Magazine*, **267**, 206-211.
17. Kandily Observatory Web Page, 2000; <http://koeri.boun.edu.tr/>.
18. Kasahara, K. (1981). "Earthquake Mechanics", Cambridge Univ. Press, Cambridge.
19. Milkereit C., Zunbul, S., Karakisa, S., Iravul, Y., and Zschau, J. (SABO Group) and Baumbach, M., Grosser, H., Gunther, E., Umutlu, N., Kuru, T., Erkul, E., Kling, K., Ibsvon Sebt, M., and Karahan, A. (Task Force) (2000). "Preliminary Aftershock Analysis of the  $M_w=7.4$  Izmit and  $M_w7.1$  Duzce Earthquake in Western Turkey, in

- A. Baraka, O. Kozaci, E. Altunel (Eds.); The 1999 Izmit and Duzce Earthquakes: Preliminary Results”, Istanbul Technical Univ. Press, Turkey.
20. Panza, G.F. and Suhadolc, P. (1987) “Complete Strong Motion Synthetics”, *Computational Technics*, **4**, Seismic Strong Motion Synthetics, ed. By B.A. Bolt, Academic Press, 153-204.
21. Tibi, R., Bock, G., Xia, Y., Baumbach, M., Grosse, H., Milkereit, C., Karakisa, S., Zunbul, Z., Kind, R., and Zschau, J. (2001). “Rupture Process of the 1999 August 17 Izmit and November 12 Duzce (Turkey) Earthquakes”, *Geophys. J. Int.*, F1-F7.
22. Zare, M. (1996). “Deux Exemple de Mouvements de Forts Seismes en Champ Proche en Iran”, *4ém Colloque National en Génie Parasismique, AFPS*, Paris, Proc. (in French), **1**, 112-119.
23. Zare, M. (1999). “Contribution à L’étude des Mouvements Forts en Iran: du Catalogue Aux Lois D’atténuation”, Université Joseph Fourier, Thèse de Doctorat (Ph.D. Thesis), 237pp.
24. Zare, M. (2000). “A Study on the Seismological and Engineering Seismological Aspects of the Izmit-Kocaeli Earthquake of 17 August 1999”, *Research Letters on Seismology and Earthquake Engineering Bulletin*, in Persian, **2**(4), 4-29.
25. Zare, M. (2001). “A Study and Processing of the Accelerometric Data of the 28 February 1997 Earthquake in Golestan, Ardebil (*Mw*6.0)”, *Research Letters on Seismology and Earthquake Engineering Bulletin*, in Persian, **4**(1), 19-33.
26. Zare, M., Bard, P-Y., and Ghafory-Ashtiany, M. (1999). “Site Characterizations for the Iranian Strong Motion Network”, *Journal of Soil Dynamics and Earthquake Engineering*, **18**(2), 101-123.

Archive of SID